Miner Petrol (2013) 107:53–65
DOI 10.1007/s00710-012-0251-5

ORIGINAL PAPER

Formation of magnesite and siderite deposits in the Southern Urals—evidence of inclusion fluid chemistry

W. Prochaska · M. Krupenin

Received: 30 July 2011 / Accepted: 12 November 2012 / Published online: 28 November 2012

Abstract World-class deposits of magnesite and siderite occur in Riphean strata of the Southern Urals, Russia. Field evidence, inclusion fluid chemistry, and stable isotope data presented in this study clearly proof that the replacement and precipitation processes leading to the formation of the epigenetic dolomite, magnesite and hydrothermal siderite were genetically related to evaporitic fluids affecting already lithified rocks. There is, however, a systematic succession of events leading to the formation of magnesite in a first stage. After burial and diagenesis the same brines were modified to hot and reducing hydrothermal fluids and were the source for the formation of hydrothermal siderite. The magnesites of the Satka Formation as well as the magnesites and the siderites of the Bakal Formation exhibit low Na/Br (106 to 222) and Cl/Br (162 to 280) ratios plotting on the seawater evaporation trend, indicating that the fluids acquired their salinity by evaporation processes of seawater. Temperature calculations based on cation exchange thermometers indicate a formation temperature of the magnesites of~130 °C. Considering the fractionation at this temperature stable isotope evidence shows that the magnesite forming brines had $\delta^{18}O_{SMOW}$ values of~+1 ‰ thus indicating a seawater origin of the original fluid. Furthermore it proves that these fluids were not yet affected by appreciable fluid-rock interaction, which again implies magnesite formation in relatively high crustal levels. In contrast to the magnesites, the siderite mineralization was caused by hydrothermal fluids that underwent more intense reactions with their host rocks in deeper crustal levels compared to the magnesite. The values of $^{87}Sr/^{86}Sr$ in the siderites are substantially higher compared to the host rock slates. They also exceed the $^{87}Sr/^{86}Sr$ ratios of the magnesites and the host rock limestones indicating these slates as the source of iron as a consequence of water-rock interaction. The siderites were formed at temperatures of~250 °C indicating a relatively heavy fluid in equilibrium with siderite of 13 ‰ $\delta^{18}O_{SMOW}$, which is in the range of diagenetic/metamorphic fluids and reflects the±complete equilibration with the host rocks. Carbon isotope evidence shows that the fluid forming the siderites underwent a much higher interaction with the host rocks resulting in a lowering of the $\delta^{13}C$ numbers (−3,3 to −3,7 ‰). The light carbon was most probably derived from decaying hydrocarbons in the Riphean sediments. In a very early stage after sedimentation of the Satka Formation (~1,550 Ma) magnesite was formed by seepage reflux of evaporitic bittern brines at the stage of riftogenic activity in the region (1,380–1,350 Ma). Sedimentation of the Bakal Formation (~1,430 Ma) and intrusion of diabase dykes (1,386±1,4 Ma) followed. Diagenetic/epigenetic mobilization of these buried fluids at~1,100 Ma resulted in the formation of hydrothermal siderite bodies.

Editorial handling: O. Thalhammer

W. Prochaska (✉)
Department of Geological Sciences, Montanuniversitaet, Leoben, Austria
e-mail: walter.prochaska@unileoben.ac.at

M. Krupenin
Institute of Geology and Geochemistry, Urals Branch of Russian Academy of Sciences, Ekaterienburg, Russia

Introduction

Investigations on the solute chemistry of inclusion fluids from hydrothermal magnesite, siderite, and their host rocks are presented in this paper in order to establish a genetic model for the magnesite and siderite mineralizations of the Southern Urals. The results from this study can be used to decipher the origin of the dissolved salt content of the fluids that precipitated magnesites and siderites, and further constrain the timing and origin of the hydrothermal event.

The chemical composition of paleofluids can be used as geochemical tracer to investigate the original signature and origin of different kinds of inclusion fluids. The chemistry

of the inclusion fluids, regarding F, Cl, Br, I, Na, K, Ca, Pb, Zn, Cu, etc., can contribute substantially to the solution of the above-mentioned problems. Regional mapping of differences in dissolved ion chemistry may provide information concerning flow directions and chemical evolution of fluids along the flow path.

Detailed investigations by Ellmies et al. (1999), Krupenin and Ellmies (2001), and Krupenin (2004) focused on stable isotope and REE chemistry and contributed substantially to the knowledge of these deposits. Nevertheless, no detailed information on the role and nature of the ore-forming fluids for the formation of the magnesite and siderite mineralizations of the Southern Urals are available. The Rb-Sr isotope systematics studied for these deposits showed different stages of the diagenetic/epigenetic ore-forming fluid-dominated processes for magnesites and siderites (Kuznetsov et al. 2005, 2007) and for pre-magnesite dolomitization of the host carbonates (Krupenin and Kuznetsov 2009).

Geologic setting of the magnesite and siderite mineralizations

Giant deposits of magnesite (Satka) and siderite/magnesite (Bakal) occur in Riphean strata of the Southern Urals. The host rocks of these deposits comprise a sedimentary sequence of up to 15 km of three different sedimentary cycles starting with clastic sediments grading into carbonate series on top of the corresponding sequence. During Late Paleozoic Uralian orogeny a foreland fold-and-thrust belt developed but generally only weak deformation affected the Proterozoic sedimentary basins. These geodynamic processes resulted in the formation of the Bashkirian Mega-Anticline (BMA), a folded and thrust megastructure in the western slope of the Southern Urals (Fig. 1). The size of this structure is about 300×100 km (Krupenin 2002).

The stratigraphic sequence of the Riphean series of the Southern Urals is shown in Fig. 2. The most important magnesite deposits of the Southern Urals are bound to the Satka Formation of the Lower Riphean with a general thickness of about 3,000 m, which is characterized by a predominance of shallow-marine carbonates, represented mainly by dolostones. The very small amount of siliciclastic materials indicates a slight relief of the hinterland. Country rocks of the mineralizations are dolostones of a shallow water marine environment that is indicated by algal mats and desiccation cracks. The Karagay Member with a thickness of about 750 m in the upper part of the Satka Formation hosts lens-shaped magnesite bodies of variable size (Fig. 3). Stratabound horizons of collapse breccias are common in the area of the magnesite mineralization (Fig. 4a–d). A series of special structural features like pseudomorphs after sulfates, tepee-structures and angle-shaped coarse-grained white dolomite, sometimes with chert in fine-grained gray dolostones, are developed in this horizon indicating evaporitic or pre-evaporitic conditions during sedimentation. Limestones occur above the magnesite-bearing level in the Kazymov Member with a thickness of about 100 m. The Pb-Pb age of this limestones is 1,550±30 Ma (Kuznetsov et al. 2007).

The stratabound Satka magnesite deposits are coarse-grained “Veitsch Type” magnesites. This very important type of magnesite is usually bound to marine platform carbonates of Proterozoic and Paleozoic age with sandstones, conglomerates and pelitic (meta-) sediments. In the Satka ore field three open pit mines and one underground mine presently produce approx. 95 % of the Russian magnesite output. The total reserves of the Satka ore field comprise about 300 million tons of raw magnesite.

On a regional scale the magnesite mineralizations are stratiform, but locally lens-shaped bodies of magnesite cut the dolomite stratification. In the Satka ore field the magnesite lenses exhibit a thickness up to 45 m with a variation in length along strike from 500 to 5,000 m (Anfimov et al. 1983). The largest ore body of the Satka orefield is the Karagay quarry, which was intensively sampled for the inclusion fluid investigations presented in this paper. As a rule, the magnesite bodies are enveloped by a dolomitic alteration zone with slightly recrystallized, fine-grained dolomite. Typically the Satka magnesites are very coarse-grained with a size of crystals up to 3 cm (in some rare occasions up to 15 cm). Magnesite is massive, banded, and of pinolitic texture. The latter is derived from the content of clay and from organic material of the host rock dolostone that is not incorporated by the newly crystallizing magnesite crystals. Rarely, relics of breccia structures can be found in the magnesite. Host rock dolomites usually exhibit sugary, fine-grained textures. Geological evidence proves magnesite formation to have taken place between the formation of the dolostones and the intrusion of crosscutting granites with Rapakivi texture; the latter have at an intrusion age of 1,370±4.6 Ma (Ronkin et al. 2007).

The siderite district of Bakal is one of the oldest mining districts in the Urals. About one billion tons of reserves are proven. The annual production decreased within the last years from 5 million tons to approximately 1 million tons. These numbers prove Bakal to be one of the world’s biggest siderite districts. The Lower Riphean Bakal Formation with a radiometric Pb-Pb age 1,430±30 Ma (Kuznetsov et al. 2003) has a thickness of about 1,500 m and comprises carbonate- and clay-dominated series hosting the siderite mineralizations. Siderite occurs in elongated stratiform bodies with an alteration halo of secondary dolomite in the four limestones and in one dolostone horizon.

Usually the siderites are fine-grained and characterized by an equigranular texture. In the inner parts of the siderite

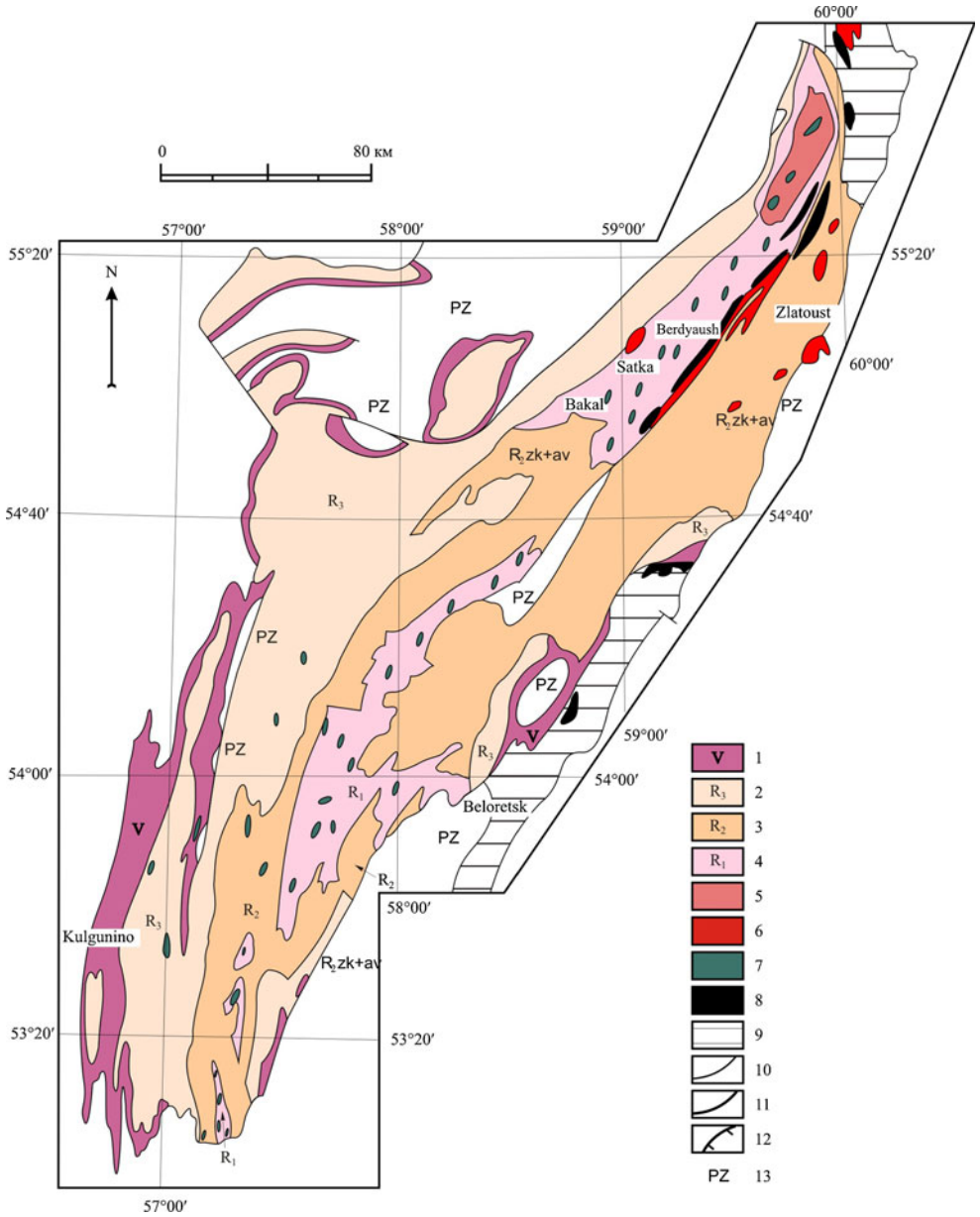

Fig. 1 Schematic geological map of the Bashkirian megaanticline. 1 – Vendian; 2 – Upper Riphean; 3 – Middle Riphean; 4 – Mashak Formation of Middle Riphean; 5 – Lower Riphean; 6 – Satka Formation of Lower Riphean; 7 – Taratash metamorphic complex (Archean – Lower Proterozoic); 8 – metamorphic complexes of Proterozoic; 9 – intrusion complexes: a – gabbroid; б – granitoid; 10 – geological boundaries; 11 – faults; 12 – thrusts; 13 – Paleozoic

bodies irregular and massive textures without any layering predominate, whereas in the peripheral parts fine-grained siderites still exhibit sedimentary textures including stromatolites etc. Figure 5a shows dolomitic stromatolites replaced by siderite still preserving the original texture. In the central parts of the siderite bodies a coarsening can be observed, and vugs filled with coarse-grained dolomite, ankerite, siderite and quartz occur (Fig. 5b).

No lithological control of this mineralization can be observed. Structural features control the distribution of the siderite bodies. Field relations clearly show that the emplacement of the basic dykes predates siderite formation. This observation is supported by the age of a diabase (1,386± 1.4 Ma, Ernst et al. 2005). The siderite-forming event, however, postdates the Early/Middle Riphean tectono-magmatic event. New Pb-Pb age data of the siderite yielded an age of 1,010±100 Ma (Kuznetsov et al. 2005). This coincides with the Middle/Late Riphean event (at the beginning of the Neoproterozoic). The deformation of the siderites can be attributed either to the Late Precambrian Cadomian event or to the Upper Paleozoic Uralian Orogeny.

Minor magnesite mineralization also occurs in the Bakal ore field. Sparry magnesite with a crystal size of about 1 cm can be found in the lower part of the dolostone horizon in the middle part of Bakal Formation (Shuidin Member). This horizon was formed in a shallow lagoon environment with stromatolite biostroms and carbonate arenite sediments. The thickness of the magnesite lenses varies from 3 up to 30 m with a variation in length from 100 to 600 m. There are 14 ore bodies with reserves of about 3.7 mt (Shevelev et al.

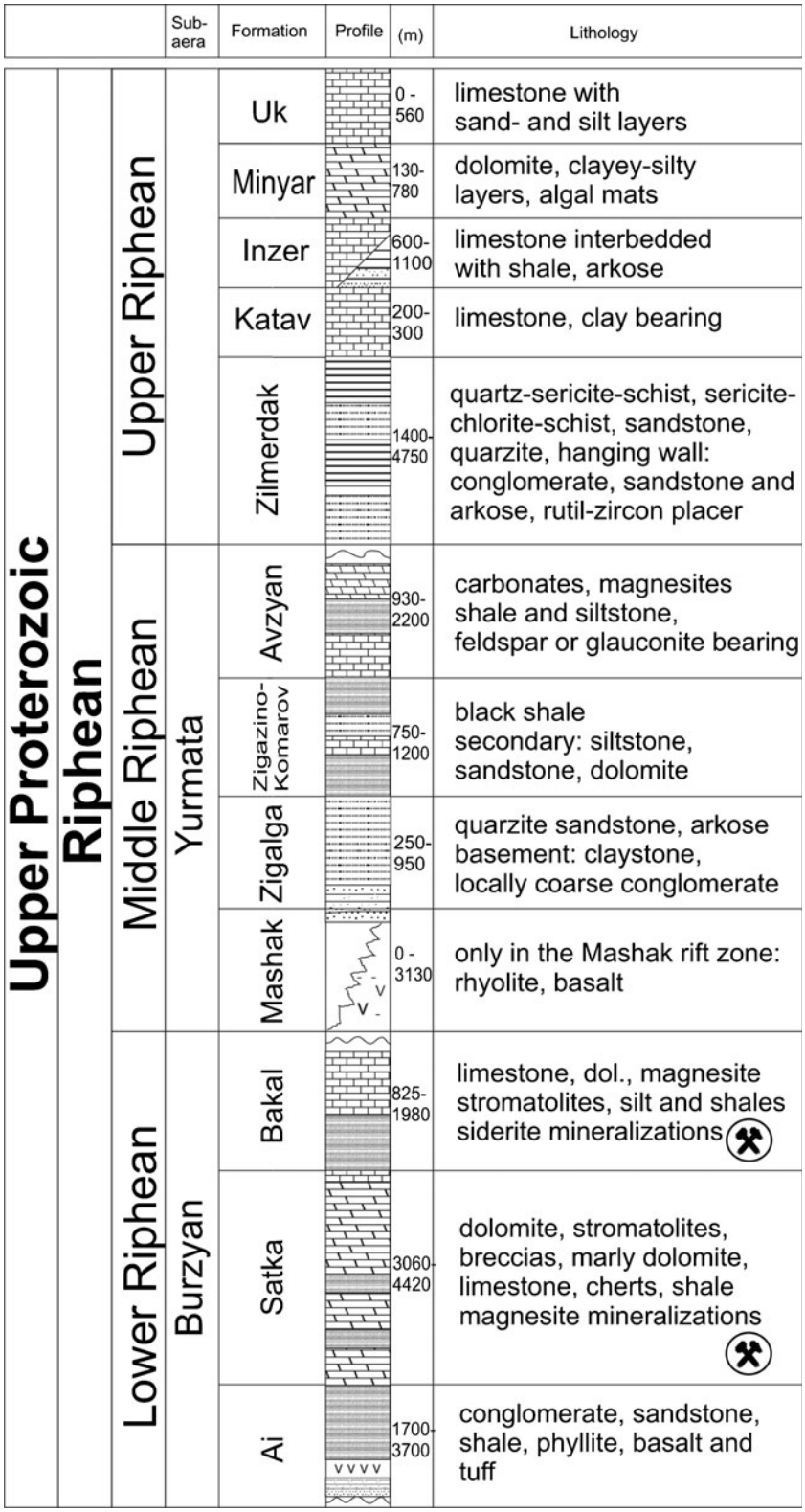

Fig. 2 Columnar profile of the Upper Proterozoic series of the Southern Urals hosting the magnesite and siderite deposits

2003). Magnesite bodies cut the bedding and stromatolite structures of the host dolomites. In the coarse-grained magnesite these structures have not been preserved. Siderite mineralization replaces the magnesite still preserving the coarse-grained magnesite structure. The occurrence of a brucite zone at the contact between the magnesite and the basic dykes shows that the formation of magnesite took place during the diagenesis of the Bakal Formation, (1,430±30 Ma, Pb-Pb age, Kuznetsov et al. 2003) and the intrusion of the diabase dykes (1,386±1.4 Ma, Ernst et al. 2005). There are

Fig. 3 Lens-shaped bodies and stocks of sparry magnesite in the Karagay quarry

local unconformities in the upper part of the magnesite bearing members in the Satka Formation and a regional unconformity above the Bakal Formation at the boundary between the Lower and Middle Riphean.

Analytical methods

Inclusion fluid chemistry

A modified technique described by Bottrell et al. (1988) was used to analyze the inclusion fluids. Inclusions in sparry magnesite, siderite, and dolomite samples were analyzed, but also fine-grained host rock limestones are suitable for the extraction of soluble salts. The samples were crushed to a grain size between 0.25 and 1 mm and carefully cleaned. 1 g of the cleaned sample and 5 ml of the leaching solution (DDW) were transferred to the thoroughly cleaned mortar and crushed.

Because of its significance for the origin of the fluids, special attention was drawn on the analyses of anions. The samples were analyzed by ion chromatography in the laboratory of the Chair of Geological Sciences at Montanuniversitaet Leoben. A Dionex system (DX-3000) with a micromembrane suppressor was used. Na, K, Li, Ca and Mg were analyzed by ion chromatography using aliquots of the same solution.

Stable isotope analysis

The stable isotope analyses were carried out in the laboratory of the Department of Earth and Atmospheric Sciences of the University of Alberta in Edmonton/Canada. For the liberation of oxygen from the analyzed samples, a modified Taylor-and Epstein-type fluorine line was used (Taylor and Epstein 1962). Fluorine gas was purified as described by Asprey (1976). Mass spectrometric analyses were carried out using a VG SIRA-9 triple collector, 90°, 9-cm-radius instrument. The analytical reproducibility of the δ-values, referred to the total analytical procedure, is in the range of 0,1 ‰. Quartz and K-feldspar standards, calibrated against NBS-28 quartz, were used for the control of the analytical results. As a reference gas, very pure CO_2, calibrated with carbonate and silicate standards, was used. Waters for hydrogen isotope analyses of fluid inclusions in carbonates were extracted by thermal decrepitation at 550 °C for 2 h. Hydrogen from the extracted fluids was generated using the zinc reduction method.

Isotope values presented are expressed in the conventional δ notation (in ‰) as $SMOW_V$ for oxygen and hydrogen. C-isotope values were normalized to PDB.

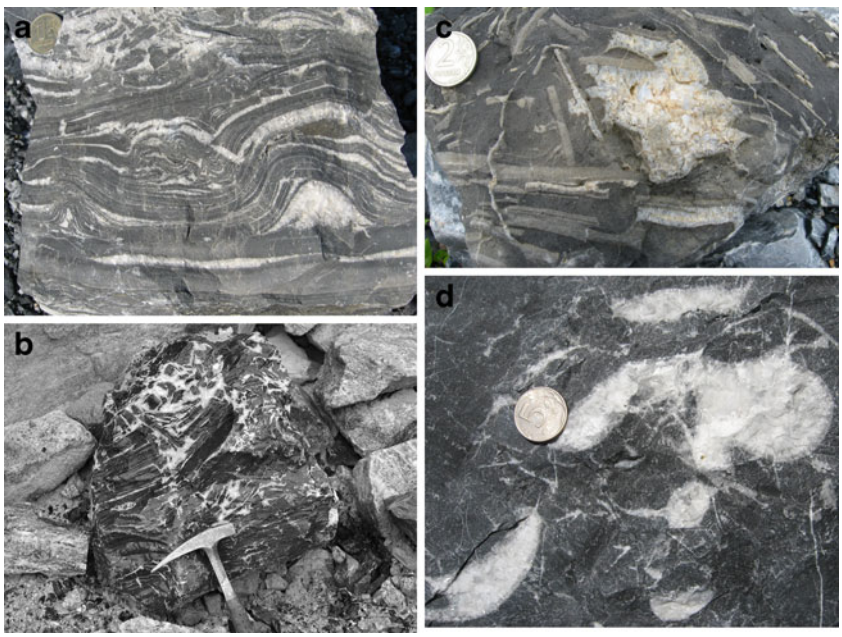

Fig. 4 Typical features indicating an early stage of evaporitic environments in the magnesite-bearing Karagay horizon of the Satka Formation: **a** Dolomite collapse breccias; **b** tepee-structure and collapse breccias filled by coarse-grained dolomite in thin bedded fine-grained dolomite; **c** sharp angle-shaped coarse-grained dolomite nest (pseudomorphs after gypsum) in dolomite collaps-breccia; **d** ellipsoid-shaped nest of coarse-grained dolomite

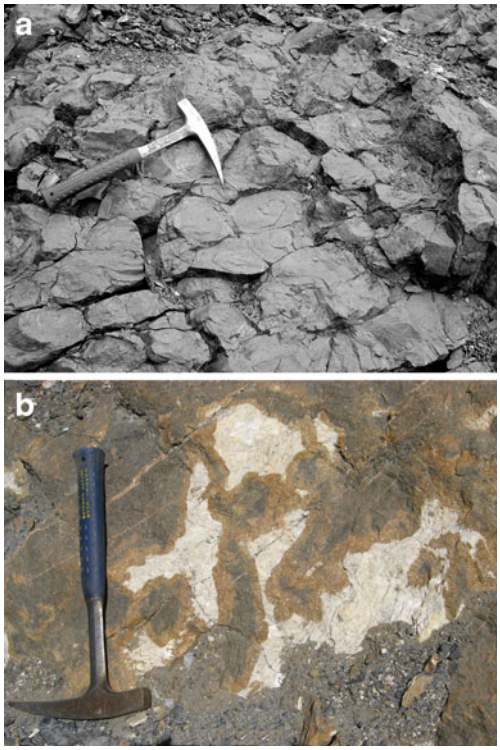

Fig. 5 Typical siderites from the Bakal deposit: **a** dolomitic stromatolites replaced by siderite still preserving the original texture; **b** siderite without primary texture, but with nests of secondary ankerite and dolomite

Inclusion fluids

Inclusion fluid chemistry

There are numerous fluid inclusions in the magnesites and consequently the total amount of fluid trapped is very high resulting in a high yield of extractable solutes. Nevertheless the size of the fluid inclusions is very small (< 5 μ) so that conventional microthermometry cannot be applied in a useful manner. This seems to be a general feature in mineralizations of sparry magnesites worldwide (e.g. Nesbitt and Prochaska 1998; Prochaska 2000). In this chapter the results of the chemical composition of the extracted inclusion fluids are presented (Table 1).

Because of the incompatible behavior of Br, changes in the molar ratios of Na/Br and Cl/Br are very sensitive for fluids being affected by evaporation processes. Fluids that have principally acquired their salinity through evaporitic concentration of seawater show Na/Br vs. Cl/Br values that are lower than seawater. In this case, the molar compositions of the fluids plot along the "evaporation trend".

Fluids which have acquired their salinity from the dissolution of halite have Na/Br vs. Cl/Br values higher than seawater and plot on the "halite dissolution trend". Surface fluids (e.g. average river water or meteoric water) are also characterized by low Br values with respect to Na and Cl.

The low Na/Br (106 to 222) and Cl/Br (162 to 280) values of the sparry magnesites and the siderites in the Lower Riphean of the Southern Urals indicate that the highly saline fluids were the product of evaporitic concentration predominantly of seawater and not of halite dissolution (Fig. 6a, b). The magnesite fluid composition (Fig. 6a) clearly lies on an evaporation trend. The Na/Br and Cl/Br ratios of the dolomitic host rocks scatter much more but are generally within the same range. This is most probably due to the incomplete equilibration of the rocks in the dolomitic alteration halo in contrast to the magnesites which are fully recrystallized and equilibrated with the mineralizing brines.

The Na/Br (90 to 199) and Cl/Br (131 to 266) values of the siderites are very similar to those of the magnesites (Fig. 6b). This suggests a common source for the magnesite as well as the siderite forming fluids. Evidently the Br-content of the fluid is not easily buffered by host rock reactions and is a relatively conservative tracer that retains its original signature even at very intense interaction of the fluid with the host rocks.

Very little is known about the geochemical behavior of iodine, and data from fluid inclusions are very rare. Iodine occurs in seawater in very low concentration. It displays a multi-oxidation-state variability and the stable form in seawater is mainly IO_3^- (Fuge 1990). Absorption of iodide by organic matter is due to the biophile behaviour of this element. In this study only I^- was analyzed.

Similar to bromine, iodine is not incorporated in the halite lattice in larger amounts. Therefore it is expected that the fractionation behavior of iodine in the evaporation process is similar to that of bromine. However, the Br/I molar ratios of the analyzed fluids of the magnesites and the siderites as well as the fluids from the dolomitic host rocks (below~500 in average) deviate drastically from seawater ratios (~ 2,000), indicating a further enrichment of iodide additional to evaporitic concentration. In the marine sedimentary Riphean limestones Br/I molar ratios are very low (< 50) and fundamentally different from the metasomatic siderites, thus reflecting a concentration of iodine in the marine sediments.

Application of chemical thermometers

Geothermometers based on semi-empirical cationic exchange reactions have originally been applied to mineralized groundwater, hot springs and geothermal wells. A review of the application of chemical thermometers was given by Kharaka and Mariner (1989).

Geothermometers based on the Na/K or Na/K/Ca ratios were successfully used by different authors (e.g. Fournier and Truesdell 1973; Fournier 1979; Giggenbach 1988; etc.). The Na/K-thermometer has overestimated the temperatures for the magnesite and especially for the siderite formation. It

Table 1 The results of the chemical analyses of the inclusion fluids. Numbers are given in ppb

	Li	Na	K	Mg	Ca	F	Cl	Br	J	SO4	Na/Br mol	Cl/Br mol
SATKA												
Magnesite												
UMS-2	12,0	7124	1027	21339	6497	151	15295	153	2,0	387	162	225
UMS-3	4,7	10445	1360	22481	771	22	21474	201	3,9	191	181	241
UMS-5	11,9	9998	1383	23413	4103	479	20362	182	5,4	225	191	252
UMS-10	6,8	10490	1585	20736	2345	47	21360	231	2,7	116	158	209
UMS-12	6,9	10829	1454	18871	919	46	23365	266	2,0	387	142	198
UMS-13	5,7	8162	1132	21925	2860	27	19123	267	2,0	274	106	162
UMS 14b	8,0	9746	1440	19859	2335	29	18761	208	1,1	238	163	203
UMS-19	5,0	10109	1294	19492	682	6	22024	268	3,7	81	131	185
UMS 22	4,9	12431	1815	28149	598	26	27597	222	1,9	111	195	280
UMS-23	2,1	5284	836	24875	2988	16	10210	83	2,8	60	222	278
UMS 27a	10,9	13442	2572	19686	1047	3	26344	298	4,2	107	157	199
UMS-28	11,9	14838	2620	15427	326	11	28887	300	11,8	169	172	217
Dolomite												
UMS-1	19,7	3186	1320	18337	12674	673	6335	27	1,1	2593	410	528
UMS-4	18,7	11023	1518	24641	10225	13	25617	246	3,3	23	156	235
UMS-6	0,4	357	151	9104	5202	119	1193	6	0,6	269	221	479
UMS-8	15,8	9605	1073	25304	11572	68	21212	141	1,2	64	236	339
UMS-9	12,7	6588	908	23936	11387	31	13534	120	2,5	53	191	255
UMS-11	6,0	3486	3622	26161	11646	194	6694	41	1,2	1604	292	364
UMS-14a	7,5	4661	882	882	9553	121	12497	101	0,5	466	161	280
UMS-15	11,2	7809	1046	1046	11031	106	19237	122	0,5	459	223	356
UMS-25	24,0	6849	1837	1837	8821	114	18026	155	4,1	69	154	263
Dolomite breccia												
UMS-16a	20,7	5967	2521	25164	12741	42	42690	489	0,8	<50	42	197
UMS 16b	70,7	21926	3748	20108	11487	11	44794	490	6,5	54	155	206
UMS-18a	13,8	5203	810	810	12482	245	11784	73	1,5	2732	249	366
UMS-18b	31,4	10525	1239	1239	12074	31	27220	246	4,9	307	149	250
UMS-20a	17,5	14258	2522	2522	11633	128	33591	347	9,3	301	143	218
UMS-20b	40,4	16797	3139	3139	10167	13	38562	349	24,2	72	167	249
UMS-26a	40,9	16358	3502	3502	10698	105	41877	345	19,4	291	165	274
UMS-26b	65,3	17154	3449	3449	11911	539	42070	389	26,1	302	153	244
UMS-26c	22,4	12510	2424	2424	7558	36	30704	298	13,3	1075	146	233
UMS 29	20,1	9351	1452	25600	10831	51	19969	169	2,5	116	193	267
UMS-51a	12,8	4039	664	22874	13571	311	7908	48	0,7	513	291	369
UMS-51b	28,9	13290	1303	24471	11569	21	25422	311	3,0	61	149	184
UMS-51c	27,0	20228	1203	6857	3786	6	33434	261	7,8	75	269	289
Chert												
UMS-27b	54,6	18227	2516	2860	1041	97	17982	129	3,6	66	491	314
UMS-54	118,3	40923	1977	1891	2168	21	61315	772	9,0	31	184	179
Calcite marble												
UMS-7	0,5	1129	846	12908	5625	255	5663	81	10,6	518	48	157
Limestone												
UMS-46	2,7	2284	492	1640	10772	35	4544	15	2,1	141	529	683
UMS-47	5,0	3155	448	1690	10509	90	5805	47	6,1	302	232	277
UMS-48	2,3	1954	388	1117	10870	51	3969	12	1,6	125	566	746

Table 1 (continued)

	Li	Na	K	Mg	Ca	F	Cl	Br	J	SO4	Na/Br mol	Cl/Br mol
BAKAL												
siderite												
UMS 33	85,7	5391	1855	9068	2268	12	12253	208	0,5	530	90	133
UMS 34	22,6	5329	1857	28181	12443	40	12758	154	0,6	1467	121	187
UMS 35a	40,4	9502	1107	19034	13073	12	19615	166	0,8	498	199	266
UMS-35b	22,7	4848	627	18182	14551	29	9768	118	0,5	78	143	187
UMS-40	31,7	5659	2878	2878	4929	53	18400	245	1,1	1630	80	169
UMS-42a	27,6	5099	5637	12882	3234	159	14560	251	1,0	1721	71	131
UMS-42b	40,2	7966	1084	10027	2082	27	18028	215	0,8	48	129	189
UMS-58	9,6	2348	1683	9855	4338	87	5365	53	0,6	467	154	227
UMS-59	12,2	3316	4354	17036	2065	145	7090	102	0,8	280	113	156
Magnesite												
UMS 31	4,0	3876	934	17797	3375	2	10045	147	2,3	176	92	154
UMS-32	17,8	4467	750	23049	11252	41	13058	224	1,3	663	69	131
UMS-44	0,8	1922	722	24156	3641	15	4877	42	2,1	59	159	262
UMS-52	7,2	2901	643	20048	11750	11	6541	59	3,0	113	171	250
Quartz												
UMS-42c	11,1	3423	865	1370	1936	25	10689	260	<0,1	30	46	93
Dolomite												
UMS 30	2,5	577	289	15674	10921	4	1242	7	0,9	18	276	385
UMS-36	13,3	3294	1330	1330	12281	36	14810	207	0,4	951	55	161
UMS-37	17,7	3240	3666	17190	14984	56	7250	92	0,4	171	122	177
UMS-39	25,5	7303	4490	18960	16263	65	23709	571	0,5	163	44	94
UMS-45	7,5	1126	619	18791	12418	144	3514	38	1,1	43	103	209
UMS-53	33,6	6517	21704	19185	16272	456	20881	293	1,3	440	77	160
Limestone												
UMS-43	41,0	9569	4996	1675	12368	118	18562	185	5,3	390	180	226
UMS 55	0,5	215	168	936	9184	185	579	1	0,7	167	523	912
UMS-56	0,3	275	136	458	10119	315	818	2	0,4	191	478	922
UMS-57	0,6	255	165	430	10755	297	908	2	1,1	188	443	1024

seems that also Mg- and Ca-based empirical geothermometers are unsuitable for calculating the temperature because the Mg- and Ca- contents of the inclusion fluids are most likely buffered by the carbonate host mineral and do not reflect the original signature of the fluids.

In this study the best and most reliable results were obtained by the Na/Li-thermometer, which was developed by Foulliac and Michard (1981) and Kharaka and Mariner (1989). The results are presented in Table 2.

The temperatures calculated from the Na/Li ratios of the inclusion fluids are consistent with the stable isotope values and other solute chemistry data and fit very well in the model discussed below. Magnesite fluids in high crustal levels were formed at relatively moderate temperatures of approximately 130 °C, while the calculated values of the siderite fluids exhibit temperatures of 250 °C consistent with the isotope data indicating a relatively low fluid rock interaction in deep crustal levels (see below).

Stable isotopes

Oxygen and carbon isotope composition

Carbon and oxygen isotope ratios of magnesite and siderite of the Southern Urals have been studied in detail and are presented in Table 3. To calculate the oxygen isotope fractionation between mineral and water, a modified increment method (Richter and Hoerness 1988) according to Schütze (1980), was used. As there are no data available for magnesite, siderite fractionation data were used. The isotopic evolution of the mineralizing fluids from seawater to magnesite

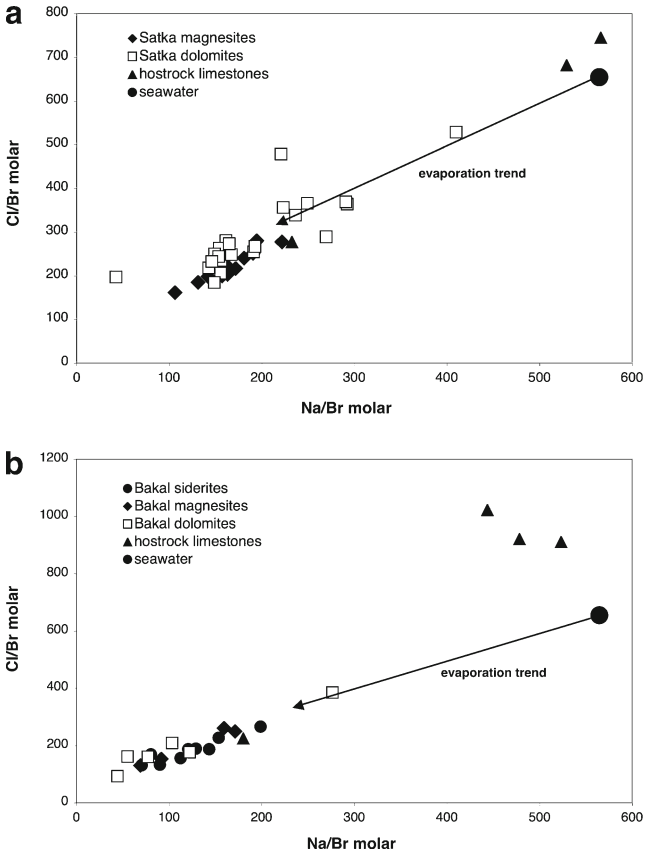

Fig. 6 **a**, **b**: Na/Br-Cl/Br molar ratios of the inclusion fluids of the mineralizations and host rocks in the Satka (**a**) and Bakal (**b**) formation

forming brines and finally to highly evolved siderite-forming hydrothermal fluids is shown in Fig. 7.

In the following the Satka magnesite and the Bakal siderite formation is considered separately on the basis of systematically distinct isotopic data.

Satka Formation A characteristic feature of the $\delta^{18}O_{SMOW}$ isotope system of the Satka samples is the difference between the magnesites (15.9 to 16.7 ‰, average: 16.1 ‰) and the host rock dolostones (19.5 to 22.1 ‰) indicating an isotopic disequilibrium between the two phases. For a temperature of 130 °C for the formation of magnesite (see the above mentioned "chemical thermometer") the calculated oxygen isotope composition of the mineralizing fluid is in the range of 1 ‰ $\delta^{18}O_{SMOW}$. Considering that evaporation processes can drive the isotopic composition of the residual brine to lighter (e.g. ~ −4 ‰) values and assume this to be the composition of the starting brine, the fluid in equilibrium with the magnesite was already modified by host rock reactions in the order of 5 ‰. Following another model which disregards fluid rock interaction the evaporative brine should have had a composition of −4 ‰ $\delta^{18}O_{SMOW}$; accordingly magnesite formation should have occurred at a temperature of approximately 90 °C. But this would mean that the calculated temperature of 130 °C from the Na-Li thermometer overestimated the formation temperatures.

Table 2 Calculated temperatures according to the Na/Li-thermometer after Foulliac and Michard (1981) and Kharaka and Mariner (1989)

Satka	
Magnesite	131,1±20,0
Dolomite	190,2±32,3
Dolomite breccia	195,7±20,4
Bakal	
Magnesite	170,5±52,0
Dolomite	239,9±16,6
Siderite	249,0±36,9

Table 3 Stable isotope ratios of the investigated rocks. δD results refer to the fluids thermally extracted from the inclusions. Isotope values presented are expressed in the conventional δ notation (in ‰) as $SMOW_V$ for oxygen and hydrogen. C-isotope values were normalized to PDB

	mineral		FI
	$\delta^{13}C_{PDB}$ (‰)	$\delta^{18}O_{SMOW}$ (‰)	δD_{SMOW} (‰)
Satka formation			
Magnesite			
UMS-2	−0,8	16,0	−50
UMS-3	−0,9	16,1	−43
UMS-10	−0,5	16,7	−46
UMS-12	−0,4	15,9	−37
Dolomite			
UMS-1	−0,6	21,5	−38
UMS-8	−0,1	21,6	−43
UMS-11	−0,7	22,1	−40
Dolomite brecia			
UMS-16a	−0,9	20,7	−57
UMS-16b	−0,7	19,5	−68
Chert			
UMS-27b		18,2	−55
UMS-54		16,6	−62
Calcite marble			
UMS-7	−2,2	19,6	−71
Limestone			
UMS-46	0,1	21,6	−26
UMS-47	0,0	22,3	−34
Bakal formation			
Siderite			
UMS-33	−3,7	21,5	−29
UMS-35a	−3,4	21,0	−38
UMS-35b	−3,3	21,1	−32
Magnesite			
UMS-32	−1,2	18,4	−44
Quartz			
UMS-42c		20,7	−65
Dolomite			
UMS-37	−2,6	21,1	−53

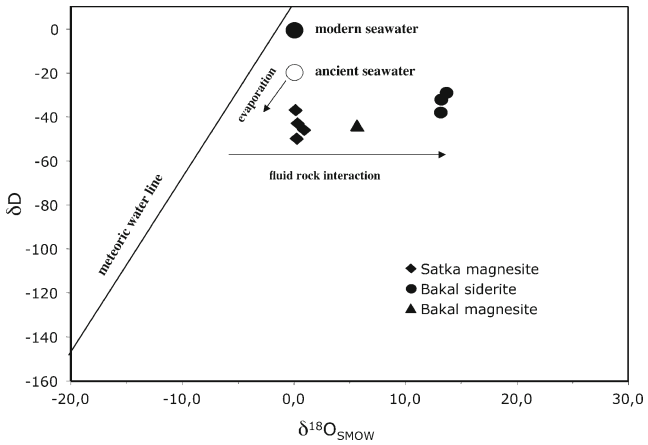

Fig. 7 δD_{SMOW} /$\delta^{18}O_{SMOW}$ diagram of the magnesite and siderite forming fluids in the Southern Urals. The fluid signature of evaporatic seawater of the magnesite forming fluids evolves towards $\delta^{18}O$-enriched diagenetic/metamorphic fluids in the siderite forming system

$\delta^{13}C_{PDB}$ values of the Satka magnesites are in a very narrow range of −0,4 to −0,8 ‰, which is totally within the range of the host rock dolostones (−0,1 to −0,9 ‰). This indicates a marine depositional environment for the carbonate hostrocks as well as seawater being the source for the mineralizing fluids. No influence of deeper crustal or mantle carbon sources can be recognized. The shift to slightly negative values possibly results from carbon generated by decomposition of hydrocarbon compounds.

Bakal Formation Generally it seems that oxygen and carbon isotope composition of the siderites and the corresponding host rock dolostones is controlled by the carbonate precursor rock. In contrast to the situation in the Satka Formation, the fluid percolating through Bakal Formation during siderite formation was buffered by reactions with the carbonate host rock and did not retain its original signature.

The $\delta^{18}O_{SMOW}$ numbers of the Bakal siderites and host rock dolostones are between 21.0 and 21.5 ‰. One magnesite sample from Bakal Formation yielded 18.4 ‰ $\delta^{18}O_{SMOW}$. Using the chemical thermometer (Na-Li-thermometer) a formation temperature of approximately 250 °C for the siderite was calculated. The corresponding fluid in equilibrium with the siderite under these conditions should have a $\delta^{18}O_{SMOW}$ composition of ~13 ‰ which means that the fluids equilibrated very well with their carbonate host rocks.

In contrast to the Satka magnesites, the siderites from Bakal Formation exhibit lighter carbon isotope composition (−3,3 to −3,7 ‰ $\delta^{13}C$). Usually these lighter $\delta^{13}C$ values are attributed to CO_2 from deep-seated sources ("average" crustal carbon) and are most probably derived from organic material in the host rock sediments.

Hydrogen isotope composition

Hydrogen isotope composition (Table 3) was included in this study because the D/H ratio is a relatively conservative and robust tracer. Like Br, the D/H ratio of a fluid migrating through the crust is not easily changed by fluid rock interaction. Studies of D/H ratios of inclusion fluids have been widely applied to investigations of hydrothermal ore formation and other crustal fluids (e.g. Magaritz and Taylor 1976; Nesbitt et al. 1986). However, this approach has not been commonly applied in studies on the origin of magnesite and siderite mineralization. Modifications of D/H ratios in sedimentary environments can be produced by the following processes: 1) admixture of meteoric fluids to seawater, 2) interaction of the fluids with rocks or organic matter, and 3) evaporitic concentration of seawater.

The hydrogen isotopes do not differ very much between the magnesites, siderites, and the host rock dolostones. The analyzed δD values of all samples are in the range of −30 to −70 ‰. Taking into account the secular variation of seawater and considering that the δD values of seawater have increased through time (Knauth and Roberts 1991) and that extensive evaporation processes drive the seawater composition to lighter values, the observed range of composition may well reflect the composition of Proterozoic evaporated seawater. There are no indications for an interaction of the fluids with maturing organic components of the host rocks (e.g. carbonate rocks with organic matter, black shales, etc.). The slightly heavier values of the siderites may reflect modification by fluid rock interaction. There is no evidence of appreciable amounts of meteoric water as a component of the original brine.

Discussion

The range in hydrogen isotope composition (−30 to −70 ‰ δD) of the fluids of the dolomite host rock, the magnesites and the siderites seems to be a possible complication with the conclusion of an evaporitic origin of the brines, given that present day seawater has a δD value of 0 ‰. A number of factors, however, could have contributed to the lowering of δD values of the original brines resulting from the evaporation of seawater. Firstly, during evaporation of seawater, δD values first rise and then decrease with increasing evaporation (Knauth and Roberts 1991), which could account for a substantial component of the low δD values in the brines. Secondly, δD values of seawater are known to have increased through time (Knauth and Roberts 1991) and consequently, the δD value of seawater in a Proterozoic lagoon would have been less than 0 ‰ prior to evaporitic concentration. Finally, in a partially closed basin, δD values of the brines in the basin are often below 0 ‰, due to influx of low

δD meteoric waters from the adjoining landmasses, which would have also lowered the initial δD values of the evaporitic brines. Nevertheless the observed δD values do not argue for meteoric influence. In the magnesite deposits of the Eastern Alps the light hydrogen isotope composition (−70 to −120 ‰ δD) is interpreted as being the result of an influx of meteoric water into a closed basin (Prochaska 2001).

Magnesite and siderite in Proterozoic series of the Southern Urals were formed in an early stage of the geodynamic evolution. Nevertheless, field observations and inclusion fluid data prove that the mineralizing processes are of epigenetic nature. It is clear from the results of this study that the replacement and precipitation processes leading to the formation of the epigenetic dolomite, magnesite, and hydrothermal siderite in the Lower Riphean carbonates of the Southern Urals were genetically related to evaporitic fluids affecting already lithified rocks. There is, however, a systematic succession of events leading to the formation of magnesite in a first stage. After burial and diagenesis the same brines were modified to hot and reducing hydrothermal fluids and were the source of the formation of hydrothermal siderite.

Formation of magnesite

A synthesis of the geological and geochemical relations of the hydrothermal dolomites and the magnesites suggest that the magnesite-forming fluids were most likely derived from evaporitic concentration of Lower Riphean seawater. However, significant quantities of evaporites cannot be found in the corresponding stratigraphic series (Krupenin 2002). Nevertheless it is possible that short episodes of arid climatic conditions dominated during Early Riphean time. Most probably the widespread brecciated dolostones with tepee-structure and sharp-angular shape of coarse-grained dolomite nests had originally been evaporitic sediments in a very shallow marine/coastal environment. Highly saline bittern brines generated in this environment descended into the subsurface resulting in dolomitization and in the formation of magnesite. The calculated $\delta^{18}O_{SMOW}$ numbers of ~1 ‰ indicate that seawater was the original fluid. Furthermore it proves that these fluids were not yet affected by appreciable fluid-rock interactions, which again implies magnesite formation at relatively high crustal levels. The carbon isotope composition is in the range of sedimentary carbonates and there is no evidence of deep crustal carbon sources. During diagenesis of the evaporitic sediments gypsum, halite, etc. were dissolved and removed, thus resulting in the formation of the observed collapse breccias. When the Mg-rich brines came into contact with the Riphean limestones (e.g. by seepage reflux), dolomite was formed in a first stage. As long as these Mg-rich brines keep coming into this system, the Mg/Ca ratios will be in the stability field of magnesite, and magnesite will be produced in favour of dolomite. At the peripheral parts close to the contact with the host rocks, a metasomatic front will move forward into the limestones as long as this process will keep going. It is hypothesized that the Mashak rifting event (1,380–1,350 Ma) initiated a high heat-flow and triggered this hydrothermal-metasomatic event.

Formation of siderite

Although the siderite forming fluids were affected by appreciable fluid-rock interaction (see below), the Na-Cl-Br-systematics of the siderite fluids still demonstrates the originally evaporitic signature because of the very conservative behaviour of Br. Formation temperatures calculated from the fluid composition and stable isotope data indicate that the formation of siderite was due to hydrothermal fluids that had more intensely interacted with their host rocks at higher temperatures in deeper crustal levels compared to the magnesite. The calculated temperature of formation of the siderites is ~250 ° C, and fluid in equilibrium with siderite under these conditions should have a $\delta^{18}O_{SMOW}$ composition of +13 ‰, which is in the range of diagenetic/metamorphic fluids and reflects the more or less complete equilibration with the host rocks.

Carbon isotope evidence also shows that the fluid forming the siderites underwent a much higher interaction with the host rocks resulting in a decrease of the $\delta^{13}C$ values (−3,3 to −3,7 ‰). The light carbon was most probably derived from decaying hydrocarbons in the Riphean sediments.

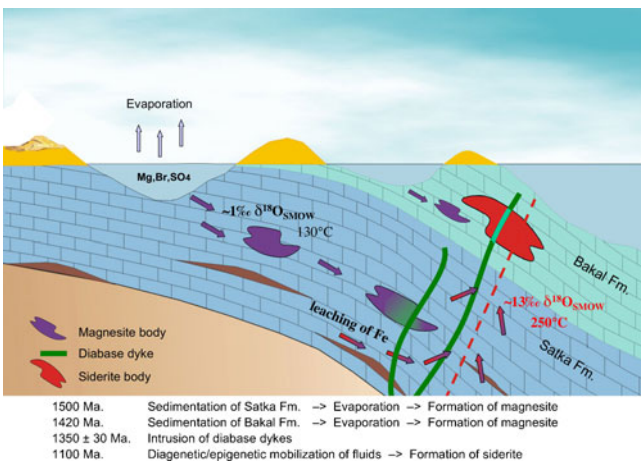

Fig. 8 Succession of events in the formation of the magnesite and siderite deposits of the Southern Urals early after the sedimentation of the Satka Formation (~ 1,550 Ma). Sedimentation of the Bakal Formation occurred at 1,420 Ma Magnesite was formed by seepage reflux of evaporitic bittern brines and was affected by the intrusion of diabase dykes at 1,350±30 Ma. Post diagenetic/epigenetic mobilization of these buried fluids at~1,100 Ma resulted in the formation of hydrothermal siderite bodies

Because of the continuous trend of the ore-forming fluids between magnesite and siderite, a consanguineous fluid for the formation of the magnesite and siderite deposits of the Southern Urals seems to be most reasonable. Only at relatively shallow crustal levels where the highly saline, Mg-rich, and Ca-depleted brines did not yet take up iron by reactions with the host rock, the fluids had the capacity for the formation of magnesite. Especially at low temperatures even extremely low Fe-contents of the fluid would prevent magnesite to be precipitated and siderite would be formed (Johannes 1970). Formation of siderite strongly depends on the depth, temperature and on the fluid rock interaction during fluid migration through the crust where the fluid had continuously been enriched in iron. In this sense siderite is only formed by highly saline, relatively hot and reducing brines in deeper crustal levels. This is in accordance with very high $^{87}Sr/^{86}Sr$ ratios of the siderites (0,735–0,739) compared to the host carbonates (0,709 in dolostones and 0,7046 in limestones, respectively). Moreover, the high $^{87}Sr/^{86}Sr$ ratios confirm the intense interaction of the fluids with pelitic host units of the Bakal Formation (Kuznetsov et al. 2005). On the contrary the much lower $^{87}Sr/^{86}Sr$ ratios (0,712–0,720) of the host rocks (dolomites and primary limestones) of the Satka magnesite indicate only minor water-rock interaction during formation of magnesite (Krupenin and Kuznetsov 2009).

Summarizing the sequence of events in the formation of the magnesite and siderite deposits of the Southern Urals, we suggest the following model: Magnesite was formed by seepage reflux of evaporitic bittern brines in an early diagenetic stages after sedimentation of Satka Formation (1,550± 30 Ma) as shown in Fig. 8. Sedimentation of the Bakal Formation (1,430±30 Ma) with a maximum thickness of about 1,500 m followed and buried the Satka sediments. There is no information so far if the formation of magnesite in the Statka and in the Bakal formation was one single process or if there were two similar subsequent processes. The intrusion of diabase dykes at 1,386±1.4 Ma clearly affected the magnesite resulting in the formation of a contact metamorphic mineral assemblage. Diagenetic/epigenetic mobilization of these buried fluids at ~1,100 Ma resulted in the formation of hydrothermal siderite deposits.

Acknowledgments The Austrian National Committee for the IGCP (project no. 443), funded fieldwork in the Urals. The laboratory work partly was funded by the Austrian Academy of Sciences. Logistic support by the Russian Academy of Sciences and funding by project SS.85.2003.5. (RAS) and 09-05-00964a (RFBR) is gratefully acknowledged.

References

Anfimov LV, Busygyn BD, Demina LE (1983) Satkinskoe magnesite deposit (South Urals). Nauka, Moscow, p 195, In Russian

Asprey LB (1976) The preparation of very pure flourine gas. J Fluor Chem 7:359–361

Bottrell SH, Yardley BWD, Buckley F (1988) A modified crush-leach method for the analysis of fluid inclusion electrolytes. Bull Mineral 111:279–290

Ellmies R, Voightlaunder G, Germann K, Krupenin MT, Moeller P (1999) Origin of giant stratabound deposits of magnesite and siderite in Riphean carbonate rocks of the Bashkir mega-anticline, western Urals. Geol Rundsch 87:589–602

Ernst RE, Pease V, Puchkov VN et al (2005) Geochemical characterization of Precambrian magmatic suites of the Southeastern margin of the East European Craton, Southern Urals, Russia. Geologicheskiy sbornik 5. IG UfSC RAS, Ufa, p 53, In Russian

Foulliac C, Michard G (1981) Sodium/lithium ratio in water applied to geothermometry of geothermal reservoirs. Geothermics 10:55–70

Fournier RO (1979) A revised equation for Na/K geothermometer. Geotherm Res Counc Trans 3:221–224

Fournier RO, Truesdell AH (1973) An empirical Na-K-Ca geothermometer for natural waters. Geochim Cosmochim Acta 37:1255–1275

Fuge R (1990) The role of volatility in the distribution of iodine in the secondary environment. Appl Geochem 5:357–360

Giggenbach WF (1988) Geothermal solute equilibria. Derivation of Na-K-Mg-Ca geoindicators. Geochim Cosmochim Acta 52:2749–2765

Johannes W (1970) Zur Entstehung von Magnesitvorkommen. N Jahb Mineral Abh 113:274–325

Kharaka YF, Mariner RH (1989) Chemical geothermometers and their application to formation waters from sedimentary basins. In: Naester ND, McCullog TH (eds) Thermal history of sedimentary basins. Springer, New York, pp 99–117

Knauth LP, Roberts SK (1991) The hydrogen and oxygen isotope history of the Silurian-Permian hydrosphere as determined by direct measurement of fossil water. In: Taylor HPJ, O'Neil JR, Kaplan IR (eds) Stable isotope geochemistry: a tribute to Samuel Epstein. Geochem Soci Spec Publ 3:91–104

Krupenin MT (2002) Comparison of Lower and Middle Riphean sparry magnesite deposits of the Southern Urals province. Spec Iss Bol Paran Geoci 50:43–50

Krupenin MT (2004) Y/Ho ratio as genetic indicator of sparry magnesites (South Urals, Russia). Acta Petrol Sin 20:803–816

Krupenin MT, Ellmies R (2001) Genetic features of sparry magnesite in Proterozoic carbonate rocks of the South Urals. In: Piestrzynski A et al (eds) Mineral deposits at the begining of the 21st century. Balkema, Lisse, pp 997–999

Krupenin MT, Kuznetsov AB (2009) Sr-isotope characteristic of magnesite and ore-hosting carbonates in type deposits from Lower Riphean of Southern Urals province. Lithosphere 5:56–71

Kuznetsov AB, Ovchinnikova GV, Gorokhov IM, Kaurova OK, Krupenin MT, Maslov AV (2003) Sr-Isotope signature and Pb–Pb age of the Bakal Formation limestones in the Lower Riphean type section, the Southern Urals. Dokl Earth Sci 391:819–822

Kuznetsov AB, Krupenin MT, Gorokhov IM, Maslov AV, Ellmies R (2005) Diagenetic transformations of Lower Riphean carbonate rocks of Bakal ore field: isotope-geochemical evidences. Lithol Miner Resour 3:227–249

Kuznetsov AB, Krupenin MT, Gorokhov IM, Maslov AV, Konstantinova GV, Kutyavin EP (2007) Strontium isotopic composition of Lower Riphean carbonate rocks in the magnesite-bearing Satka Formation, Southern Urals. Dokl Earth Sci 414:599–604

Magaritz M, Taylor HPJ (1976) $^{18}O/^{16}O$ and D/H studies along a 500 km traverse across the Coast Range batholith and its country rocks, central British Columbia. Can J Earth Sci 13:1514–1536

Nesbitt B, Prochaska W (1998) Solute chemistry of inclusion fluids from sparry dolomites and magnesites in Middle Cambrian

carbonate rocks of the Southern Canadian Rocky Mountains. Can J Earth Sci 35:546–555

Nesbitt BE, Murowchick JB, Muehlenbachs K (1986) Dual origins of lode gold deposits in the Canadian Cordillera. Geology 14:506–509

Prochaska W (2000) Magnesite and talc deposits in Austria. Miner Slovac 32:543–548

Prochaska W (2001) Magnesite mineralizations of the Eastern Alps and the Carpathians. In: Piestrzynski A et al (eds) Mineral deposits at the beginning of the 21st century. Balkema, Lisse, pp 1017–1019

Richter R, Hoernes S (1988) The application of the increment method in comparison with experimentally derived and calculated O-isotope fractionations. Chem Erde 48:1–18

Ronkin YL, Maslow AV, Kazak AP et al (2007) Boundary between lower and middle Riphean, Southern Urals: new isotope U-Pb-SHRIMP-II contingencies. Dokl Earth Sci 415:319–322

Schütze H (1980) Der Isotopenindex—Eine Inkrementenmethode zur näherungsweisen Berechnung von Isotopenaustauschgleichgewichten zwischen kristallinen Substanzen. Chem Erde 39:321–334

Shevelev A, Zuev L, Fedorov V (2003) The raw material base of magnesite and brucite of Russia. CJC "Novoe znanie", Kazan, p 162, In Russian

Taylor RP, Epstein S (1962) Relation between oxygen isotope ratios in coexisting minerals of igneous and metamorphic rocks. I. Principles and experimental results. Bull Geol Soc Am 73:461–480